Continuous-discrete trajectory PHD and CPHD filters

Ángel F. García-Fernández[⋆∘], Simon Maskell[⋆]
[⋆]Dept. of Electrical Engineering and Electronics, University of Liverpool, United Kingdom
[∘]ARIES Research Center, Universidad Antonio de Nebrija, Spain
Emails: {angel.garcia-fernandez, s.maskell}@liverpool.ac.uk

***Abstract*—This paper presents the continuous-discrete trajectory probability hypothesis density (CD-TPHD) and the continuous-discrete trajectory cardinality PHD (CD-TCPHD) filter. We consider continuous-time models for target appearance, dynamics and disappearance, which are discretised to obtain the corresponding continuous-discrete models. The CD-TPHD filter propagates a Poisson point process approximation to the posterior (multi-trajectory) density over the set of alive trajectories sampled at the time instants when the measurements have been taken. The CD-TCPHD filter proceeds analogously but propagating a density on an independent and identically distributed (IID) cluster process. An important, novel feature of these filters is that they can infer the time of appearance and the state at appearance time of the trajectories in continuous time, not being constrained to discretised time steps.**

***Index Terms*—Multiple target tracking, sets of trajectories, probability hypothesis density, continuous-discrete systems.**

I. Introduction

Multiple target tracking (MTT) is concerned with the estimation of the trajectories of the targets that appear, move, and disappear from a scene of interest based on a sequence of noisy measurements [1], [2]. The ability to solve MTT problems is important in numerous applications, for example, unmanned surface vehicles [3], autonomous driving [4] and air traffic monitoring [5]. There are several ways of addressing the MTT problem: for example using the random finite set (RFS) formulation [6], multiple hypothesis tracking [1] and the joint integrated probabilistic data association filter [7]. Links between these approaches are established in [8], [9].

The standard multi-target dynamic models include target birth, single target dynamic and death models given in discrete time, at the time steps when the measurements are taken [6]. That is, these models do not consider continuous models for target appearance, movement and disappearance. Continuous models are important, as they decouple the multi-target dynamic modelling from the measurement sampling time. They have the advantage that, with the same underlying continuous time multi-target model, one can compare several systems with different sampling times. In addition, continuous multi-target dynamic models are particularly important to design filters when the time interval between measurements is not fixed [10].

In [10], a continuous-discrete multi-target model is proposed. In this model, the time of target appearance and disappearance is given by an $\mathrm{M}/\mathrm{M}/\infty$ queuing system [11], as in [12]–[14]. This queuing system implies that the time of appearance is modelled as a Poisson point process (PPP) in time, and target life span is exponentially distributed. In addition, the continuous time model considers that targets move independently according to a stochastic differential equation (SDE) [15] and that, at the time of appearance, targets have a known spatial distribution. The resulting discretisation results in a standard continuous-discrete multi-target dynamic model, in which targets survive and move independently with Markovian dynamics, and the birth process is a PPP.

For PPP birth, as required in continuous-discrete filtering, and the standard measurement and dynamic models, the solution to the multi-target filtering problem is given by the Poisson multi-Bernoulli mixture (PMBM) filter [16]–[18]. The true PMBM posterior can be approximated by propagating a PPP density through the filtering recursion, which is done by performing Kullback-Leibler divergence (KLD) minimisations at the update step [19]. The resulting filter is the probability hypothesis density (PHD) filter. Another possibility is to propagate an independent and identically distributed (IID) cluster process density instead of a PPP. In this case, KLD minimisations are required after the prediction and the update step [16], [20]. The resulting filter is the cardinality PHD (CPHD) filter [21]. Even though the PHD and CPHD filters have a low performance compared to the PMBM filter [17], they are filters of interest due to their low computational complexity and acceptable performance in many applications [22]–[26], and they are the focus in this paper.

One of the drawbacks of the PHD/CPHD filters, in discrete [19] and continuous-discrete form [10], is that they do not provide information on the target trajectories, as the considered posterior only contains information on the current set of targets. Solutions based on tagging Gaussian components in Gaussian mixture implementations [27], [28] are not guaranteed to work well, as each Gaussian component actually represents information over many potential targets [29]. This drawback of PHD/CPHD filtering can be solved by considering (multi-trajectory) densities over sets of trajectories instead of sets of targets [30]. The posterior density over the sets of trajectories contains all available information over the target trajectories, and is also PMBM [31], [32]. The PHD/CPHD filters that approximate posterior density on sets of trajectories are referred to as trajectory PHD/CPHD (TPHD/TCPHD) filters [29]. The TPHD/TCPHD filters propagate a PPP density and an IID cluster density, respectively, on the set of alive trajectories through the filtering recursion by performing the corresponding KLD minimisations. Due to the considered PPP and IID cluster approximation, the TPHD/TCPHD filter posterior approximations are only useful to estimate the trajectories of the alive targets at the current time steps.

In this work, we develop the continuous-discrete TPHD/TCPHD filters. In order to do so, we first define sets of trajectories that are discretised at the times when the measurements are taken. Then, we use the continuous-discrete multi target model in [10] to directly obtain these filters. In addition, we derive the form of the posterior densities adding the information on the appearance time and state of the trajectories in continuous time, not being constrained to discretised time steps. To our knowledge, this is a novel feature of this work, not present in previous multitarget filters.

II. Problem formulation

We consider the problem of estimating target trajectories when the models for target appearance, movement and disappearance are in continuous time and we take measurements at some discrete time steps. In particular, we want to estimate the trajectories of the targets that are present in the surveillance area at the current time.

The multi-target state at time t, where $t \in [0,\infty)$, is represented by set $\mathbf{x}(t) \in \mathcal{F}(\mathbb{R}^{n_x})$, where $\mathbb{R}^{n_x}$ is the single target space, and $\mathcal{F}(\mathbb{R}^{n_x})$ is the space of all finite subsets of $\mathbb{R}^{n_x}$. At any time t, targets may appear and disappear from $\mathbf{x}(t)$. These models will be discussed in Section III.

At known time instants t_k, $k \in \mathbb{N} \cup \{0\}$ we take noisy measurements of the multi-target state $\mathbf{x}_k = \mathbf{x}(t_k)$. In this paper, we refer to k as the time step k, which corresponds to a time t_k. The measurements are modelled by the standard point target measurement model [6]. That is, at time step k, we observe a set $\mathbf{z}_k \in \mathcal{F}(\mathbb{R}^{n_z})$ of measurements, which contains target-generated measurements as well as clutter. Given $\mathbf{x}_k$, each target $x \in \mathbf{x}_k$ is detected with probability $p_D(x)$ and generates a measurement with conditional density $l(\cdot|x)$, or missed with probability $1-p_D(x)$. The clutter process is independent from the target-generated measurements and is a PPP with intensity $\lambda^C(\cdot)$. Set $\mathbf{z}_k$ is the union of the set of target-generated measurements and set of clutter measurements.

A. Sets of trajectories

In order to be able to estimate target trajectories using a Bayesian approach, we will consider multi-trajectory densities on sets of trajectories [30]. We proceed to define how trajectories and sets of trajectories are considered in continuous-discrete systems, and the corresponding set integral.

We consider target trajectories up to the current time t_k sampled at the times when the measurements are taken. That is, a target trajectory is defined by its initial time step $\beta \in \{0,1,...,k\}$, its length υ, which corresponds to the number of time steps that the trajectory has been present and, its sequence $x^{1:\nu} = \left(x^1,...,x^\upsilon\right)$ of states at the time steps in which it has been alive, i.e., from time step β to time step $\beta+\nu-1$. A trajectory up to time step k is therefore represented as a variable $\left(\beta, x^{1:\nu}\right)$, where (β,ν) belongs to the set $I_{(k)} = \{(\beta,\nu) : 0 \le \beta \le k \,\text{and}\, 1 \le \nu \le k-\beta+1\}$, which ensures that that the beginning and end of the trajectory belong to the considered time window.

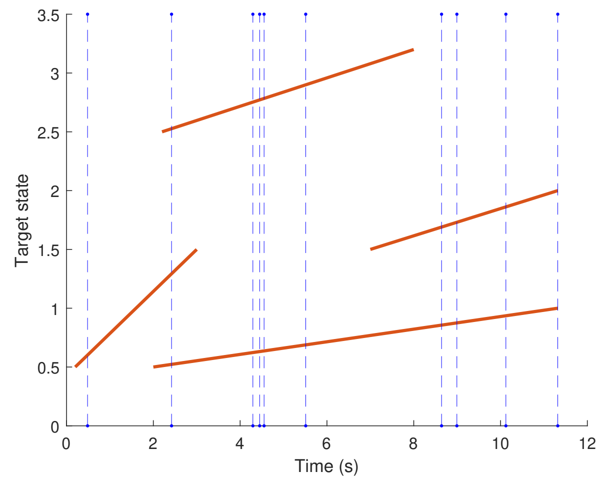

Figure 1: Illustration of a set of one-dimensional trajectories in continuous time and its discretisation. The set has four trajectories shown as red lines. The vertical dashed lines indicate the times at which measurements have been taken. The trajectories are discretised at these time steps.

A single trajectory X up to time step k therefore belongs to the space $T_{(k)} = \uplus_{(\beta,\nu)\in I_{(k)}} \{\beta\} \times \mathbb{R}^{\nu n_x}$, where $\uplus$ stands for disjoint union, which is used to highlight that the sets are disjoint. Similarly to the set $\mathbf{x}$ of targets, we denote a set of trajectories up to time step k as $\mathbf{X} \in \mathcal{F}\left(T_{(k)}\right)$.

Example 1. We consider one-dimensional targets and the four trajectories in continuous time shown in Figure 1. We have received measurements asynchronously at the times indicated by the vertical dashed lines. The continuous trajectories are discretised at these time steps to obtain a set of trajectories $\mathbf{X} \in \mathcal{F}\left(T_{(k)}\right)$. For example, the trajectory that appears first is (approximately) represented in discretised form as $(1,(0.6,1.29))$. This means that it appears at the time of the first round of measurements with a state 0.6, has a duration of two time steps, defined according to the measurements, and at time step two has a state 1.29. The discretised version of the rest of the trajectories is obtained analogously.

In addition, considering that the last vertical dash line represents the current time, there are two trajectories that have already disappeared and two trajectories that are alive. In TPHD/TCPHD filtering, we are concerned with estimating the alive trajectories [29]. □

B. Integration

We first consider integrals in the single trajectory space $T_{(k)}$. For a real-valued function $\pi(\cdot)$ on $T_{(k)}$, its integral is [30]

$$\int \pi(X)\,dX = \sum_{(\beta,\nu)\in I_{(k)}} \int \pi\left(\beta, x^{1:\nu}\right) dx^{1:\nu}. \tag{1}$$

It should be noted that the integral sums over all possible start times and lengths, and integrates the corresponding target states. Then, we can directly obtain the set integral as follows.

Given a real-valued function $\pi(\cdot)$ on the space $\mathcal{F}\left(T_{(k)}\right)$ of sets of trajectories, its set integral is [30]

$$\int \pi(\mathbf{X})\,\delta\mathbf{X} = \sum_{n=0}^{\infty} \frac{1}{n!} \int \pi(\{X_1, ..., X_n\})\, dX_{1:n} \quad (2)$$

where $X_{1:n} = (X_1, ..., X_n)$. A function $\pi(\cdot)$ is a multitrajectory density if $\pi(\cdot) \geq 0$ and its set integral is one.

III. Continuous-discrete multi-target models

We consider the continuous-discrete multi-target model in [10], which we proceed to review. To distinguish between target births and deaths in continuous and discrete time, we refer to target births and deaths in continuous time as target appearances and disappearances, and use the terms births and deaths for the discretised system.

A. Continuous time model

The continuous multi-target model is characterised by

- A1 The times of target appearances is a Poisson process (in time) with rate λ [11].
- A2 When a target appears, its distribution is independent of the rest of the targets and is Gaussian with mean $\overline{x}_a$ and covariance matrix P_a.
- A3 The life span τ of a target is independent and exponentially distributed with rate μ.
- A4 Targets move independently following a linear time invariant SDE [15]

  $$dx(t) = Ax(t)\,dt + Ld\beta(t) \quad (3)$$

  where $x(t) \in \mathbb{R}^{n_x}$ is the target state at time t, A and L are matrices, $dx(t)$ is the differential of $x(t)$, and $\beta(t) \in \mathbb{R}^{n_\beta}$ is a Brownian motion, also called Wiener process, with diffusion matrix Q_β. The size of matrices A and L are $n_x \times n_x$ and $n_x \times n_\beta$, respectively.

It should be noted that we use β to denote a trajectory birth time and $\beta(t)$ to denote a Brownian motion.

B. Continuous-discrete model

The above continuous multi-target model can be discretised at the times when the measurements are taken to obtain a standard multi-target dynamic model [6]. That is, in the resulting discretised multi-target model, given the current multi-target state, each target survives to the next time step independently of the rest with a certain (time dependent) probability of survival, each surviving target moves independently of the rest with a transition density, and new targets are born following a PPP birth process.

We consider the evolution of the system from time t_{k-1} to t_k and denote $\Delta t_k = t_k - t_{k-1}$. The discretised system has a probability of survival

$$p_{S,k} = e^{-\mu \Delta t_k}. \quad (4)$$

The single target transition density $g_k(\cdot|\cdot)$ is [15]

$$g_k(x(t_k)\,|x(t_{k-1})) = \mathcal{N}(x(t_k); F_k x(t_{k-1}), Q_k) \quad (5)$$

$$F_{(\Delta t_k)} = \exp(A\Delta t_k) \quad (6)$$

$$Q_{(\Delta t_k)} = \int_0^{\Delta t_k} \exp(A(\Delta t_k - \xi))\, L Q_\beta L^T \times \exp(A(\Delta t_k - \xi))^T d\xi \quad (7)$$

where $\exp(A)$ denotes the matrix exponential of A and $\mathcal{N}(x; \overline{x}, Q)$ denotes a Gaussian density with mean $\overline{x}$ and covariance matrix Q evaluated at x. We also denote $F_k = F_{(\Delta t_k)}$ and $Q_k = Q_{(\Delta t_k)}$.

The birth model is a PPP with intensity

$$D_k^B(x_k) = \frac{\lambda}{\mu}\left(1 - e^{-\mu \Delta t_k}\right) \int_0^{\Delta t_k} p_k(x_k\,|t)\, p_k(t)\, dt \quad (8)$$

where

$$p_k(x_k\,|t) = \mathcal{N}\left(x_k; F_{(t)}\overline{x}_a, F_{(t)} P_a F_{(t)}^T + Q_{(t)}\right) \quad (9)$$

$$p_k(t) = \frac{\mu}{1 - e^{-\mu \Delta t_k}} e^{-\mu t} \chi_{[0, \Delta t_k)}(t) \quad (10)$$

where $\chi_A(t)$ is the indicator function of set A evaluated at t: $\chi_A(t) = 1$ if $t \in A$ and $\chi_A(t) = 0$ otherwise.

Density (10) is a truncated exponential distribution with parameter μ in the interval $[0, \Delta t_k)$ and represents the density of the time lag t of new born targets. That is, if a target appears at time step $t_k - t$ with $t \in [0, \Delta t_k)$, then t denotes the time lag between appearing time and t_k. Density (9) represents the single target density at time step t_k given that the target appeared with a time lag t. Algorithm 1 indicates how to sample the set of trajectories up to the current time in the continuous-discrete multi-target system.

Algorithm 1 Sampling the set of all trajectories (alive and dead) in the continuous-discrete system.

Input: Time instants $t_1, ..., t_K$, models in A1-A4.
Output: Set $\mathbf{X}_K$ of trajectories up to time step K.

```
- Initialisation X_0 = ∅, t_0 = 0.
for k = 1 to K do
    - Δt_k = t_k − t_{k−1}.
    - X_k = ∅.                                   ▷ Initialisation at time step k.
    for all X = (β, x^{1:ν}) ∈ X_{k−1} do        ▷ Go through previous trajectories.
        if β + ν − 1 < k − 1 then                ▷ Trajectory is dead.
            - X_k = X_k ∪ {X}.
        else                                     ▷ Trajectory is alive.
            - Set s = 1 with probability p_{S,k}, (4), s = 0, otherwise.
            if s = 1 then                        ▷ Trajectory X survives.
                - Sample y ~ g_k(y |x^ν), see (5).
                - Set X_k = X_k ∪ {(β, x^{1:ν}, y)}.
            else                                 ▷ Trajectory X does not survive.
                - Set X_k = X_k ∪ {X}.
            end if
        end if
    end for
    - Sample n from a Poisson distribution with mean (λ/μ)(1 − e^{−μΔt_k}).
    for i = 1 to n do                            ▷ Go through new born targets.
        - Sample t from (10).
        - Sample x_k from p_k(x_k |t), see (9).
        - Set X_k = X_k ∪ {(k, x_k)}.
    end for
end for
```

IV. Continuous-discrete TPHD and TCPHD filters

TPHD and TCPHD filters provide an approximation to the posterior on the alive set of trajectories [29], by recursively minimising the corresponding KLD minimisations, as explained in the introduction. Once we have obtained the continuous-discrete system parameters, it is straightforward to obtain the continuous-discrete TPHD and TCPHD filters. That is, the continuous-discrete TPHD and TCPHD filters are given by the TPHD and TCPHD filtering recursions [29] using the birth model (8), probability of survival (4), and single target transition density (5). We proceed to review the most relevant aspects of the filters so that in the next section we can explain how to include information on time and state of appearance.

A. PPP and IID cluster densities on sets of trajectories

In this section, we review the PPP and IID cluster densities on sets of trajectories [29], as these are the types of densities TPHD/TCPHD filtering considers. A PPP on sets of trajectories has a cardinality that is Poisson distributed and its elements are IID. Its density is of the form

$$\pi\left(\{X_1,...,X_n\}\right)=e^{-\lambda_\pi}\lambda_\pi^n\prod_{j=1}^{n}\breve{\pi}\left(X_j\right) \tag{11}$$

where $\lambda_\pi \geq 0$, $\breve{\pi}(\cdot)$ is a single trajectory density, which implies

$$\int\breve{\pi}\left(X\right)dX=1. \tag{12}$$

A PPP with density $\pi(\cdot)$ can be characterised by λ_π and $\breve{\pi}(\cdot)$, or by its intensity $D_\pi(\cdot)$, also called probability hypothesis density (PHD), which is a function on the single trajectory space and is given by

$$D_\pi\left(X\right)=\lambda_\pi\breve{\pi}\left(X\right). \tag{13}$$

An IID cluster density has an arbitrary cardinality distribution and, given the cardinality, its elements are IID. An IID cluster density is of the form

$$\pi\left(\{X_1,...,X_n\}\right)=\rho_\pi\left(n\right)n!\prod_{j=1}^{n}\breve{\pi}\left(X_j\right) \tag{14}$$

where $\rho_\pi(\cdot)$ is the cardinality distribution and $\breve{\pi}(\cdot)$ is a single trajectory density, so it meets (12). An IID cluster density is characterised by $\rho_\pi(\cdot)$ and $\breve{\pi}(\cdot)$, and also by $\rho_\pi(\cdot)$ and its PHD

$$D_\pi\left(X\right)=\breve{\pi}\left(X\right)\left(\sum_{n=0}^{\infty}n\rho_\pi\left(n\right)\right) \tag{15}$$

where the factor within the parenthesis in (15) represents the expected number of trajectories. How to obtain samples from these two types of densities on sets of trajectories is explained in the supplementary material of [29].

B. Gaussian mixture implementations

In this section, we briefly explain the Gaussian mixture implementation of the CD-TPHD and CD-TCPHD filters for the Wiener velocity model (also called nearly constant velocity model), which arises from an SDE of the form (3) [10], [15]. We first introduce the notation for a Gaussian density, with known birth time step and length, on the single trajectory space

$$\mathcal{N}\left(\beta,x^{1:\nu};\overline{\beta},m,P\right)$$
$$=\begin{cases}\mathcal{N}\left(x^{1:\nu};m,P\right) & \beta=\overline{\beta},\,\nu=\overline{\nu}\\ 0 & \text{otherwise}\end{cases} \tag{16}$$

where $\overline{\nu}=\dim\left(m\right)/n_x$. Equation (16) represents a single trajectory Gaussian density with birth time step $\overline{\beta}$, length $\overline{\nu}$, mean $m\in\mathbb{R}^{\overline{\nu}n_x}$ and covariance matrix $P\in\mathbb{R}^{\overline{\nu}n_x\times\overline{\nu}n_x}$ evaluated at trajectory $\left(\beta,x^{1:\nu}\right)$.

The PHD of the corresponding PPP or IID cluster density is represented as a Gaussian mixture on sets of trajectories. That is, the PHD of the alive set of trajectories at time step $k'\in\{k,k+1\}$ given the measurements up to time step k is

$$D_{k'|k}\left(X\right)=\sum_{j=1}^{J_{k'|k}}w_{k'|k}^{j}\mathcal{N}\left(X;\beta_{k'|k}^{j},m_{k'|k}^{j},P_{k'|k}^{j}\right) \tag{17}$$

where $J_{k'|k}$ is the number of Gaussian components, and $w_{k'|k}^{j}$, $\beta_{k'|k}^{j}$, $m_{k'|k}^{j}$ and $P_{k'|k}^{j}$ represent the weight, start time, mean and covariance matrix of the j-th component, respectively. In addition, $\sum_{j=1}^{J_{k'|k}}w_{k'|k}^{j}$ represents the expected number of alive trajectories, as it corresponds to the integral of the PHD [29].

The Gaussian mixture implementations of the TPHD and TCPHD filters require the following types of models

- A1 $p_{S,k}$ and p_D do not depend on the state.
- A2 $g_k\left(x^i\left|x^{i-1}\right.\right)=\mathcal{N}\left(x^i;F_kx^{i-1},Q_k\right)$.
- A3 $l\left(z|x\right)=\mathcal{N}\left(z;Hx,R\right)$.
- A4 The PHD of the target birth process is Gaussian or Gaussian mixture.

From Section III-B, we know $p_{S,k}$ and $g_k\left(\cdot|\cdot\right)$ have the required form. However, the PHD of the target birth (8) is non-Gaussian. The technique to be able to derive Gaussian implementations of continuous-discrete multiple target filters is to carry out a KLD minimisation on the birth process to obtain a PHD of the desired form. In fact, for the Wiener velocity model, we can obtain the resulting PPP in closed-form, see [10, Prop. 2]. With this result, one can directly extend the Gaussian mixture TPHD/TCPHD filtering recursions to the continuous-discrete case.

Due to page length constraints, we refer to the reader to [29] to check the specifics of the Gaussian mixture implementations of the TPHD and TCPHD filters. Practical implementations of these recursions require some approximations with the following parameters: pruning threshold Γ_p to discard PHD components with low weight, maximum number J_{max} of PHD components, absorption threshold Γ_a (which is an operation for single-trajectory densities related to merging), and size of the L-scan window (to discard trajectory correlations outside the last L time steps).

1) Estimation: As in PHD/CPHD filtering for sets of targets, there are many ways of estimating the set of alive trajectories at each time step from a PPP or IID cluster posterior. One method for each filter is explained in [29, Sec. VI.D]. These methods first determine the number $\hat{n}_k$ of estimated trajectories, and then report the set of trajectories made up of the means of the PHD components (which include birth time step, length and sequence of states) with $\hat{n}_k$ highest weights. That is, the estimated set of alive trajectories is

$$\hat{\mathbf{X}}_k=\left\{\left(\beta_{k|k}^{l_1},m_{k|k}^{l_1},\right),...,\left(\beta_{k|k}^{l_{\hat{n}_k}},m_{k|k}^{l_{\hat{n}_k}}\right)\right\}$$

where $\{l_1, ..., l_{\hat{n}_k}\}$ are the indices of the PHD components with highest weights. We recall that this set of trajectories is sampled at the times when measurements have been taken. In the next section, we will explain how we can also estimate the time and state of appearance in continuous time.

V. Inference on appearance time and state

The continuous-discrete TPHD and TCPHD filters provide information on the alive trajectories sampled at the time steps when the measurements have been taken. In this section, we go one step further and obtain the information corresponding to the appearance time and state of the trajectories. That is, due to the continuous time model, we are not constrained to the measurement sampling process to infer when and where targets entered the area of interest.

Example 2. We consider again the example in Figure 1. The trajectory that appears last is born with a state 1.69 at time step 7, which corresponds to time 8.64 s. Nevertheless, this trajectory actually appeared at a time 7 s with a state 1.5. In this section, we indicate how to obtain probabilistic information on this event using the continuous-discrete TPHD and TCPHD filters. □

We also motivate the potential applications of this type of inference with a simplified illustrative example.

Example 3. Let us consider we want to estimate the times when certain animals enter an area next to a river. There is prior information on the rate at which animals enter this area to drink, the time they spend in the area, and their dynamics. A monitoring system observes the scene sporadically. Prior information is of help to make more accurate estimations of appearance times, not being limited by the sampling process of the monitoring system. □

A. Single trajectory case

Given a single trajectory $X = \left(\beta, x^{1:\nu}\right)$, its time of birth (which is defined at the sampled times) is t_β, which corresponds to time step β. We want to infer its time lag of appearance t and state x^0 at appearance time. Its time lag of appearance is directly related to appearance time $t_a = t_\beta - t$.

From A2, we know that

$$p\left(x^0|t\right) = \mathcal{N}\left(x^0; \overline{x}_a, P_a\right).$$

In addition, the distribution of the time lag is given by $p_\beta\left(t\right)$, see (10). Therefore, the joint prior density of x^1, x^0, t is

$$\begin{aligned} p\left(x^1, x^0, t\right) &= \mathcal{N}\left(x^1, F_{(t)}x^0, Q_{(t)}\right) \\ &\quad \times \mathcal{N}\left(x^0; \overline{x}_a, P_a\right) p_\beta\left(t\right) \end{aligned} \tag{18}$$

where the distribution of the time lag is independent of x^1, x^0. Then, the density of x^0, t given x^1 is

$$g_0\left(x^0, t|x^1\right) = p_\beta\left(t\right) g_0\left(x^0|x^1, t\right)$$

where

$$\begin{aligned} g_0\left(x^0|x^1, t\right) &= \mathcal{N}\left(x^0; \overline{x}_a + G_{(t)}\left(x^1 - F_{(t)}\overline{x}_a\right), P_{u,(t)}\right) \\ G_{(t)} &= P_a F_{(t)}^T \left(F_{(t)} P_a F_{(t)}^T + Q_{(t)}\right)^{-1} \\ P_{u,(t)} &= P_a - G_{(t)} F_{(t)} P_a. \end{aligned}$$

Note that, due to the Gaussian distributions in (18), the conditional distribution $g_0\left(x^0|x^1, t\right)$ is obtained by the Kalman filter update, with an appropriate selection of parameters [33].

Then, if X has a distribution $p\left(X\right)$, the density on the augmented trajectory $\widetilde{X} = \left(t, \beta, x^{0:\nu}\right)$, which includes time lag t of appearance and target state x^0 at appearance time, is

$$p\left(t, \beta, x^{0:\nu}\right) = p\left(\beta, x^{1:\nu}\right) g_0\left(x^0|x^1, t\right) p\left(t\right).$$

B. Transition density to augmented trajectory

Given a trajectory $X = \left(\beta', y^{1:\nu'}\right)$, its transition density to an augmented trajectory $\widetilde{X} = \left(t, \beta, x^{0:\nu}\right)$ is

$$g_0\left(\widetilde{X}|X\right) = g_0\left(x^0|y^1, t\right) p_{\beta'}\left(t\right) \delta_{\beta'}\left[\beta\right] \delta_{\nu'}\left[\nu\right] \delta_{y^{1:v'}}\left[x^{1:v}\right].$$

As targets appear at independent times with independent spatial distributions, the transition density for sets of trajectories to sets of augmented trajectories is [30, App. C]

$$g_0\left(\left\{\widetilde{X}_1, ..., \widetilde{X}_n\right\} | \left\{X_1, ..., X_n\right\}\right) = \sum_{\sigma \in \Gamma_n} \prod_{j=1}^{n} g_0\left(\widetilde{X}_{\sigma_j} | X_j\right) \tag{19}$$

where Γ_n is the set that includes all the permutations of $(1, ..., n)$ and $\sigma = (\sigma_1, ..., \sigma_n)$.

C. Incorporating appearance information into an IID cluster

We consider an IID cluster density $\pi\left(\cdot\right)$ on sets of trajectories, see (14). The density $\widetilde{\pi}\left(\cdot\right)$ on the augmented trajectories is given by the Chapman-Kolmogorov equation using the transition density (19) and the IID cluster density (14)

$$\widetilde{\pi}\left(\widetilde{\mathbf{X}}\right) = \int g_0\left(\widetilde{\mathbf{X}} | \mathbf{X}\right) \pi\left(\mathbf{X}\right) \delta\mathbf{X}.$$

The calculation of this set integral directly yields

$$\begin{aligned} &\widetilde{\pi}\left(\left\{\left(t_1, \beta_1, x_1^{0:\nu_1}\right), ..., \left(t_n, \beta_n, x_n^{0:\nu_n}\right)\right\}\right) \\ &\quad = \rho_\pi\left(n\right) n! \prod_{j=1}^{n} \left[\breve{\pi}\left(\beta_j, x_j^{0:\nu_j}\right) p_{\beta_j}\left(t_j\right) g_0\left(x_j^0|x_j^1, t_j\right)\right]. \end{aligned}$$

That is, given an IID cluster RFS on the set of trajectories, the distribution on the set of augmented trajectories, is also an IID cluster with the same cardinality distribution. Each single trajectory density is augmented independently. As the PPP is a particular case of the IID cluster, this also implies that, given a PPP on the set of trajectories, the distribution on the set of augmented trajectories is a PPP (with the same expected number of trajectories). This implies that from the posterior approximation provided by the CD-TPHD and CD-TCPHD filters, we can directly obtain the posterior that also includes information on appearance time and state.

D. Estimation for Gaussian distributions

As mentioned in Section IV-B1, we perform trajectory estimation in the Gaussian mixture implementations of the TPHD/TCPHD filters using the PHD components (single-trajectory densities) with highest weights. We proceed to explain how to additionally estimate the appearance time and state for Gaussian single-trajectory densities. Given a density

$$p\left(t,\beta,x^{0:\nu}\right)=\mathcal{N}\left(\beta,x^{1:\nu};\beta^{k},m^{k},P^{k}\right)g_{0}\left(x^{0}|x^{1},t\right)p_{\beta}\left(t\right),$$

we estimate the augmented trajectory $\left(\hat{t},\hat{\beta},\hat{x}^{0:\hat{\nu}}\right)$ as

$$\begin{aligned}\hat{\beta}&=\beta^{k}\\ \hat{\nu}&=\dim\left(m^{k}\right)/n_{x}\\ \hat{t}&=\mathrm{E}\left[t|\hat{\beta}\right]=\frac{1}{\mu}-\frac{\Delta t_{\hat{\beta}}e^{-\mu\Delta t_{\hat{\beta}}}}{1-e^{-\mu\Delta t_{\hat{\beta}}}}\\ \hat{x}^{0:\hat{\nu}}&=\mathrm{E}\left[x^{0:\nu}|\hat{\beta},\hat{\nu},\hat{t}\right]\\ &=\left[\begin{array}{c}\overline{x}_{a}+G_{(\hat{t})}\left(m_{1}^{k}-F_{(\hat{t})}\overline{x}_{a}\right)\\ m^{k}\end{array}\right]\end{aligned}$$

where m_1^k is the target state at time of birth of m^k (its first n_x components).

VI. Simulations

We proceed to evaluate the proposed CD-TPHD and CD-TCPHD filters via simulations. A target state at time t_k is $x\left(t_k\right)=\left[p_1\left(t_k\right),p_2\left(t_k\right),v_1\left(t_k\right),v_2\left(t_k\right)\right]^T$, which comprises position and velocity of a target moving in a 2-D plane. The target moves with a Wiener velocity model, such that

$$F_{(t)}=\left(\begin{array}{cc}I_2 & tI_2\\ 0_2 & I_2\end{array}\right),\quad Q_{(t)}=q\left(\begin{array}{cc}\frac{t^3}{3}I_2 & \frac{t^2}{2}I_2\\ \frac{t^2}{2}I_2 & tI_2\end{array}\right)\tag{20}$$

where q is the diffusion coefficient of the driving Brownian motion [15].

We consider the following parameters for the system dynamics: $\lambda=0.10\,\mathrm{s}^{-1}$, $\mu=0.0015\,\mathrm{s}^{-1}$, $q=0.2\,\mathrm{m}^2/\mathrm{s}^3$. The mean and covariance matrix at appearance time are given by

$$P_a\overline{x}_a=\left[\overline{p}_a^T,\overline{v}_a^T\right]^T,\quad P_a=\left(\begin{array}{cc}P_a^{pp} & P_a^{pv}\\ \left(P_a^{pv}\right)^T & P_a^{vv}\end{array}\right)\tag{21}$$

where $\overline{p}_a=[250,200]^T$ (m), $\overline{v}_a=[3,0]^T$ (m/s), $P_a^{pp}=\mathrm{diag}\left(\left[80^2,80^2\right]\right)\left(\mathrm{m}^2\right)$, $P_a^{vv}=\mathrm{diag}\left([1,1]\right)\left(\mathrm{m}^2/\mathrm{s}^2\right)$ and $P_a^{pv}=0_2\left(\mathrm{m}^2/\mathrm{s}\right)$. At time $t_0=0$, the probability that there are zero targets is one. As $\mu=0.0015\,\mathrm{s}^{-1}$, the average life span of a target is 666.7 s and in stationary regime, the average number of targets is $\frac{\lambda}{\mu}=6.67$.

We take 100 measurements, and the time interval between measurements Δt_k has been sampled from an exponential distribution with parameter $\mu_m=1\,\mathrm{s}^{-1}$. We consider the same time intervals as in [10, Fig. 2]. The considered ground truth set of trajectories, which contains 12 trajectories and was obtained by Algorithm 1, is shown in Figure 2. Figure 2 also shows the number of alive trajectories at each time step.

We measure target position with parameters

$$H=\left[I_2\quad 0_2\right],\quad R=\sigma_r^2I_2$$

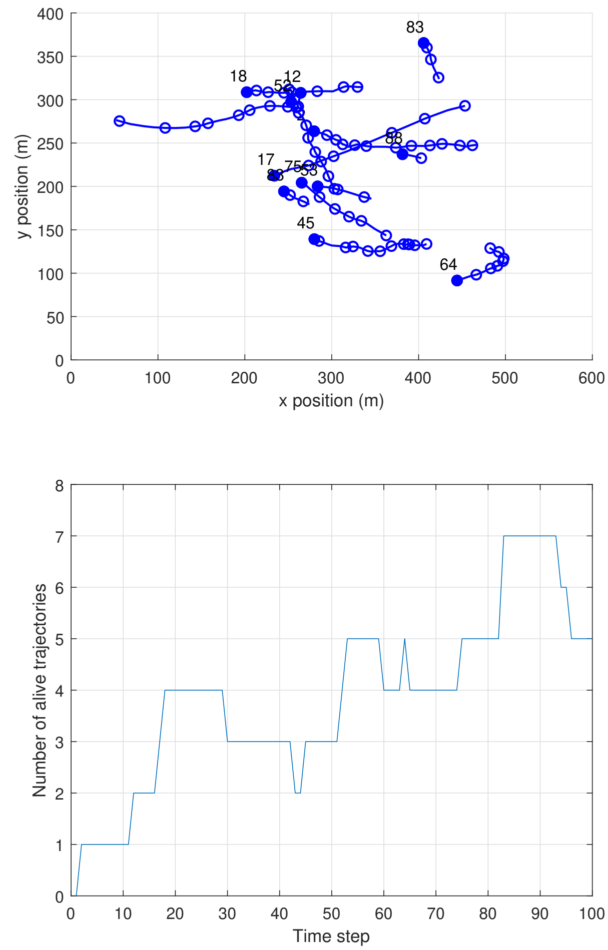

Figure 2: Ground truth set of trajectories (top) and number of alive trajectories at each time step (bottom). The positions of a trajectory every ten time steps is indicated by circles, which is filled for the position at time of birth. Time step of birth is indicated next to the initial position.

where $\sigma_r^2=4\,\mathrm{m}^2$, $p_D=0.9$ and $\lambda^C\left(z\right)=\lambda_c\cdot u_A\left(z\right)$ where $u_A\left(z\right)$ is a uniform density in the area $A=[0,600]\times[0,400]$ and $\lambda_c=10$.

At each time step, the CD-TPHD and CD-TCPHD filters are used to estimate the set of alive trajectories, sampled at the time steps when measurements have been taken. In addition, for both filters, it is possible to recover the information regarding time of appearance and target state at time of appearance, which happens before the time of birth, as was indicated in Section V-D. An illustration of how this property, which is a distinctive characteristic of continuous-discrete multiple target trackers based on sets of trajectories, is shown in Figure 3.

We have implemented the L-scan Gaussian mixture implementations of the CD-TPHD and CD-TCPHD filters[1] with $L\in\{1,2,5\}$ [29]. These filters also use the following parameters: pruning threshold $\Gamma_p=10^{-5}$, absorption threshold $\Gamma_a=4$ and maximum number of PHD components $J_{max}=30$. We evaluate the performance of the filters by Monte Carlo

[1]Matlab implementations of the TPHD and TCPHD filters are available at https://github.com/Agarciafernandez/MTT.

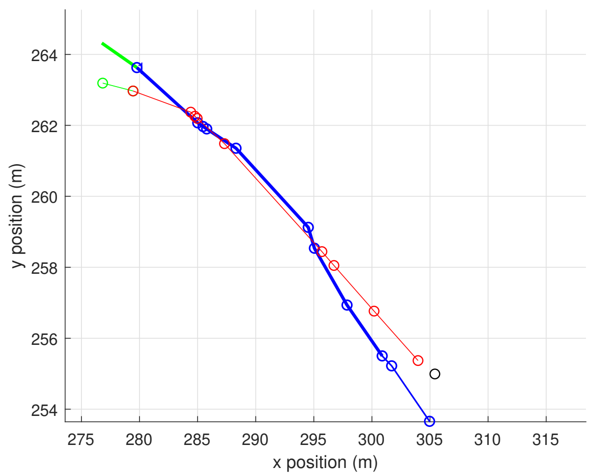

Figure 3: Exemplar trajectory estimation including its state at appearance time. The figure shows a zoom of one trajectory and its estimate, provided by the CD-PHD filter, at time step $k = 10$. The black circle is a current measurement at time step 10. The blue line is the true trajectory and there is a circle marking its position at each time step. The blue line is thicker to highlight the part of the trajectory that corresponds to past or current target states. The appended green line represents the part of the trajectory before target birth, that is, the end point corresponds to its position at appearance time. The red line represents the estimated trajectory ($\hat{\beta} = 2$) via CD-TPHD filtering, where the red dots represents the trajectory position at each time step. The appended green line and circle represent the estimated target position at appearance time, which is obtained using the procedure in Section V-D.

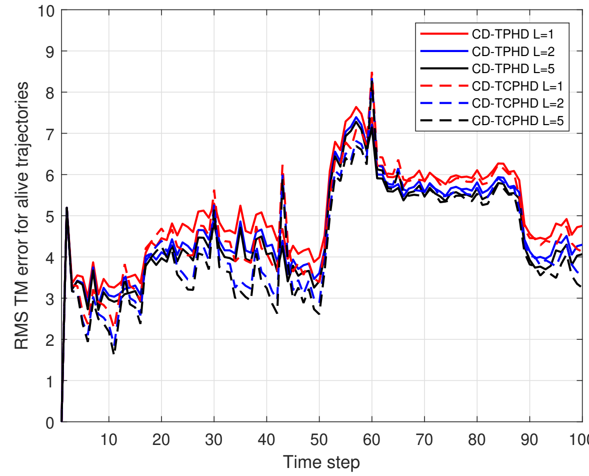

Figure 4: Trajectory metric error of the continuous-discrete filters to estimate the alive trajectories at each time step. The CD-TCPHD filter outperforms the CD-TPHD filter and accuracy improves by increasing the window length L.

simulation with $N_{mc} = 100$ runs. At each time step k, we obtain the error between the true set $\mathbf{X}_k$ of alive trajectories, which is represented in Figure 2, and the estimated set $\hat{\mathbf{X}}_k$ of alive trajectories, provided by the CD-TPHD and CD-TCPHD filters. We measure this error by using the trajectory metric (TM), which is defined for sets of trajectories, based on linear programming in [34] with parameters $p = 2$, $c = 10$ and $\gamma = 1$. We the denote the TM as $d(\cdot,\cdot)$, and we will use that $d^2(\cdot,\cdot)$ can be decomposed into the square costs: $c_m^2(\cdot,\cdot)$ for missed targets, $c_f^2(\cdot,\cdot)$ for false targets, $c_l^2(\cdot,\cdot)$ for the localisation error of properly detected targets, and $c_s^2(\cdot,\cdot)$ for track switches. That is, we have

$$d^2\left(\mathbf{X}_k, \hat{\mathbf{X}}_k\right) = c_l^2\left(\mathbf{X}_k, \hat{\mathbf{X}}_k\right) + c_m^2\left(\mathbf{X}_k, \hat{\mathbf{X}}_k\right) + c_f^2\left(\mathbf{X}_k, \hat{\mathbf{X}}_k\right) + c_s^2\left(\mathbf{X}_k, \hat{\mathbf{X}}_k\right). \quad (22)$$

In the presented results, we only use the position elements to compute the trajectory metric and normalise the error by the considered time window. The resulting root mean square (RMS) error at a given time step is calculated as

$$d(k) = \sqrt{\frac{1}{N_{mc}k}\sum_{i=1}^{N_{mc}} d^2\left(\mathbf{X}_k, \hat{\mathbf{X}}_{k,i}\right)}, \quad (23)$$

where $\hat{\mathbf{X}}_{k,i}$ is the estimated set of alive trajectories at time k in the ith Monte Carlo run.

The TM errors for the two algorithms and $L \in \{1, 2, 5\}$ are shown in Figure 4. We can see that the CD-TCPHD slightly outperforms the CD-TPHD filter. In addition, the error decreases by increasing L, as the filters are able to improve the estimation of previous time steps. A more thorough analysis can be provided by the plots of the decomposed errors in (22), which are shown in Figure 5. We can first see that for a given L, the CD-TPHD and CD-TCPHD filters produce the same localisation error. An increase in L lowers the localisation error, but has negligible effect on the other costs. The CD-TCPHD filter is better at missing fewer targets between time steps 20 and 60 than the CD-TPHD. We can also see that the increase in the error that there is from around time step 50 to 90 is due to an increase in the false target cost. In addition, in this time window, there is also some track switching. The track switching is created by a target that is born at close distance from a previously existing trajectory.

As, in this scenario, the CD-TPHD and CD-TCPHD filters estimates have very low track switching costs, see Figure 5, the resulting TM errors are quite similar to the errors computed by the sum of the generalised optimal sub-pattern assignment (GOSPA) metric ($\alpha = 2$) [35] between the set of true targets and the estimated set of targets across all time steps (which would correspond to the trajectory metric for $\gamma \to 0$).

VII. Conclusions

We have proposed the continuous-discrete trajectory PHD and CPHD filters. These filters are based on continuous-time multi-target models that are discretised at the times when measurements are taken. Both filters consider (multi-trajectory) densities on the set of trajectories of the alive targets, where the trajectories are sampled at the measurement time stamps. As the TPHD filter, the continuous-discrete TPHD filter obtains a PPP density approximation to the posterior over the set of trajectories by minimising the KLD at each update step. Similarly, as the TCPHD filter, the continuous-discrete TCPHD filter propagates an IID cluster density approximation through the filtering recursion by performing KLD minimisations at the prediction and update steps.

A distinct and novel feature of these filters is that they can estimate the appearance time and state of the trajectories in

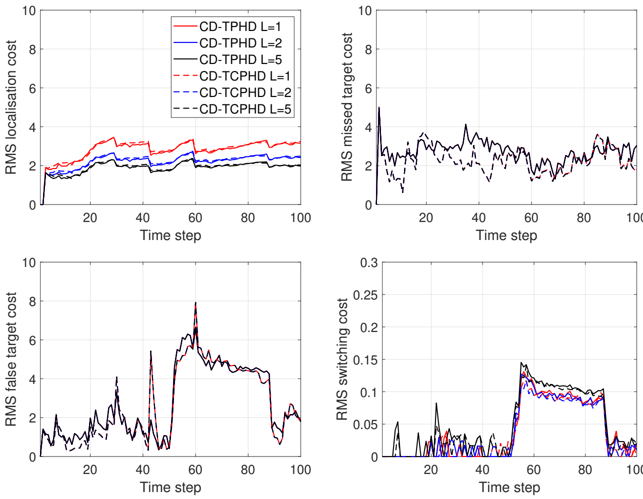

Figure 5: Decomposition of the trajectory metric into localisation error for properly detected targets, costs for missed targets, costs for false targets and track switching costs. The switching costs are quite small in comparison with the other costs.

continuous time, not being constrained to previously discretised time steps. Future work includes the extension of these filters to non-linear SDEs [15].

REFERENCES

[1] S. Blackman and R. Popoli, *Design and Analysis of Modern Tracking Systems*. Artech House, 1999.

[2] S. Challa, M. R. Morelande, D. Musicki, and R. J. Evans, *Fundamentals of Object Tracking*. Cambridge University Press, 2011.

[3] E. F. Brekke, E. F. Wilthil, B.-O. H. Eriksen, D. K. M. Kufoalor, Ø. K. Helgesen, I. B. Hagen, M. Breivik, and T. A. Johansen, "The Autosea project: Developing closed-loop target tracking and collision avoidance systems," *Journal of Physics: Conference Series*, vol. 1357, pp. 1–12, Oct. 2019.

[4] J. Honer and H. Hettmann, "Motion state classification for automotive LIDAR based on evidential grid maps and transferable belief model," in *21st International Conference on Information Fusion*, July 2018, pp. 1056–1063.

[5] C. Hurter, N. H. Riche, S. M. Drucker, M. Cordeil, R. Alligier, and R. Vuillemot, "FiberClay: Sculpting three dimensional trajectories to reveal structural insights," *IEEE Transactions on Visualization and Computer Graphics*, vol. 25, no. 1, pp. 704–714, Jan. 2019.

[6] R. P. S. Mahler, *Advances in Statistical Multisource-Multitarget Information Fusion*. Artech House, 2014.

[7] D. Musicki and R. Evans, "Joint integrated probabilistic data association: JIPDA," *IEEE Transactions on Aerospace and Electronic Systems*, vol. 40, no. 3, pp. 1093–1099, July 2004.

[8] J. L. Williams, "Marginal multi-Bernoulli filters: RFS derivation of MHT, JIPDA and association-based MeMBer," *IEEE Transactions on Aerospace and Electronic Systems*, vol. 51, no. 3, pp. 1664–1687, July 2015.

[9] E. Brekke and M. Chitre, "Relationship between finite set statistics and the multiple hypothesis tracker," *IEEE Transactions on Aerospace and Electronic Systems*, vol. 54, no. 4, pp. 1902–1917, Aug. 2018.

[10] A. F. García-Fernández and S. Maskell, "Continuous-discrete multiple target filtering: PMBM, PHD and CPHD filter implementations," *IEEE Transactions on Signal Processing*, vol. 68, pp. 1300–1314, 2020.

[11] L. Kleinrock, *Queueing Systems*. John Wiley & Sons, 1976.

[12] S. P. Coraluppi, C. A. Carthel, and A. S. Willsky, "Multiple hypothesis tracking and graph-based tracking extensions," *Journal of Advances in Information Fusion*, vol. 14, no. 2, pp. 152–166, Dec. 2019.

[13] S. Coraluppi and C. A. Carthel, "If a tree falls in the woods, it does make a sound: multiple-hypothesis tracking with undetected target births," *IEEE Transactions on Aerospace and Electronic Systems*, vol. 50, no. 3, pp. 2379–2388, July 2014.

[14] A. F. García-Fernández, J. Grajal, and M. R. Morelande, "Two-layer particle filter for multiple target detection and tracking," *IEEE Transactions on Aerospace and Electronic Systems*, vol. 49, no. 3, pp. 1569–1588, July 2013.

[15] S. Särkkä and A. Solin, *Applied Stochastic Differential Equations*. Cambridge University Press, 2019.

[16] J. L. Williams, "An efficient, variational approximation of the best fitting multi-Bernoulli filter," *IEEE Transactions on Signal Processing*, vol. 63, no. 1, pp. 258–273, Jan. 2015.

[17] A. F. García-Fernández, J. L. Williams, K. Granström, and L. Svensson, "Poisson multi-Bernoulli mixture filter: direct derivation and implementation," *IEEE Transactions on Aerospace and Electronic Systems*, vol. 54, no. 4, pp. 1883–1901, Aug. 2018.

[18] Y. Xia, K. Granström, L. Svensson, and A. F. García-Fernández, "Performance evaluation of multi-Bernoulli conjugate priors for multi-target filtering," in *20th International Conference on Information Fusion*, July 2017, pp. 1–8.

[19] R. P. S. Mahler, "Multitarget Bayes filtering via first-order multitarget moments," *IEEE Transactions on Aerospace and Electronic Systems*, vol. 39, no. 4, pp. 1152–1178, Oct. 2003.

[20] A. F. García-Fernández and B.-N. Vo, "Derivation of the PHD and CPHD filters based on direct Kullback-Leibler divergence minimization," *IEEE Transactions on Signal Processing*, vol. 63, no. 21, pp. 5812–5820, Nov. 2015.

[21] R. Mahler, "PHD filters of higher order in target number," *IEEE Transactions on Aerospace and Electronic Systems*, vol. 43, no. 4, pp. 1523–1543, Oct. 2007.

[22] Z. Fu, F. Angelini, J. Chambers, and S. M. Naqvi, "Multi-level cooperative fusion of GM-PHD filters for online multiple human tracking," *IEEE Transactions on Multimedia*, vol. 21, no. 9, pp. 2277–2291, Sep. 2019.

[23] C. Lundquist, L. Hammarstrand, and F. Gustafsson, "Road intensity based mapping using radar measurements with a probability hypothesis density filter," *IEEE Transactions on Signal Processing*, vol. 59, no. 4, pp. 1397–1408, April 2011.

[24] M. Üney, D. E. Clark, and S. J. Julier, "Distributed fusion of PHD filters via exponential mixture densities," *IEEE Journal of Selected Topics in Signal Processing*, vol. 7, no. 3, pp. 521–531, June 2013.

[25] G. Battistelli, L. Chisci, C. Fantacci, A. Farina, and A. Graziano, "Consensus CPHD filter for distributed multitarget tracking," *IEEE Journal of Selected Topics in Signal Processing*, vol. 7, no. 3, pp. 508–520, June 2013.

[26] J. Mullane, B.-N. Vo, M. D. Adams, and B.-T. Vo, "A random-finite-set approach to Bayesian SLAM," *IEEE Transactions on Robotics*, vol. 27, no. 2, pp. 268–282, April 2011.

[27] Z. Lu, W. Hu, and T. Kirubarajan, "Labeled random finite sets with moment approximation," *IEEE Transactions on Signal Processing*, vol. 65, no. 13, pp. 3384–3398, July 2017.

[28] K. Panta, D. Clark, and B.-N. Vo, "Data association and track management for the Gaussian mixture probability hypothesis density filter," *IEEE Transactions on Aerospace and Electronic Systems*, vol. 45, no. 3, pp. 1003–1016, July 2009.

[29] A. F. García-Fernández and L. Svensson, "Trajectory PHD and CPHD filters," *IEEE Transactions on Signal Processing*, vol. 67, no. 22, pp. 5702–5714, Nov 2019.

[30] A. F. García-Fernández, L. Svensson, and M. R. Morelande, "Multiple target tracking based on sets of trajectories," *accepted for publication in IEEE Transactions on Aerospace and Electronic Systems*, 2019. [Online]. Available: https://arxiv.org/abs/1605.08163

[31] K. Granström, L. Svensson, Y. Xia, J. Williams, and A. F. García-Fernández, "Poisson multi-Bernoulli mixtures for sets of trajectories," 2019. [Online]. Available: https://arxiv.org/abs/1912.08718

[32] Y. Xia, K. Granström, L. Svensson, A. F. García-Fernández, and J. L. Wlliams, "Multi-scan implementation of the trajectory Poisson multi-Bernoulli mixture filter," *Journal of Advances in Information Fusion*, vol. 14, no. 2, pp. 213–235, Dec. 2019.

[33] S. Särkkä, *Bayesian Filtering and Smoothing*. Cambridge University Press, 2013.

[34] A. S. Rahmathullah, A. F. García-Fernández, and L. Svensson, "A metric on the space of finite sets of trajectories for evaluation of multi-target tracking algorithms," 2016. [Online]. Available: http://arxiv.org/abs/1605.01177

[35] ——, "Generalized optimal sub-pattern assignment metric," in *20th International Conference on Information Fusion*, 2017, pp. 1–8.